Publishing House
AKAPIT

COMPUTER METHODS IN MATERIALS SCIENCE

Informatyka w Technologii Materiałów

Vol. 11, 2011, No. 3

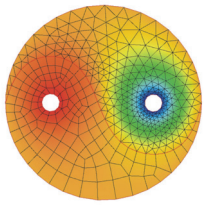

APPLICATION OF A POPULATION BALANCE MODEL FOR PREDICTION OF BEHAVIOUR OF NON-METALLIC INCLUSIONS IN THE LIQUID STEEL

ADAM CWUDZIŃSKI, JAN JOWSA

Czestochowa University of Technology, Faculty of Materials Processing Technology and Applied Physics, Department of Metals Extraction and Recirculation, Armii Krajowej 19 ave, 42-200 Czestochowa, Poland
**Corresponding author: cwudzinski@wip.pcz.pl*

Abstract

The article presents the results of computer simulations of steel flow in a one-strand tundish with low dam. The authors employed the CFD (Computational Fluid Dynamics) numerical modeling technique to demonstrate the effect of different variants of boundary and initial conditions on the numerical result of steel flow and behaviour of non-metallic inclusions (NMI). The computer simulations were performed for non-isothermal, steady and non-steady conditions. To predict of behaviour non-metallic inclusions in the liquid steel "mixture" model and "population balance" model were used. As a result of computations, NMI size distribution curve, RTD curves and the percentage shares of particular flow zones (stagnant flow, plug flow, and ideal mixing flow) were obtained.

Key words: numerical modeling, tundish, steel flow, non-metallic inclusions, NMI size distribution curve, RTD curves

1. INTRODUCTION

Mathematical modelling of metallurgical processes is a dynamically developing technique for studying phenomena determining the course of chemical reactions between the components of liquid steel. In steel metallurgy processes, where metallurgical reactions are stimulated mechanically (e.g. as a result of blowing in an inert gas), the hydrodynamics of liquid metal motion within the plant concerned is gaining increasing importance. One of the steel metallurgy plants is the tundish which is used in the continuous steel casting process. The flow of liquid steel in the tundish can be influenced by installing additional flow control devices e.g. dams or weirs in its working space (Ahn et al., 2007; Liu et al., 2008). Gas-permeable barriers can also be used with a good effect on the flow hydrodynamics by blowing in argon gas to the liquid steel (Zhong et al., 2008; Cwudziński & Jowsa, 2008a). During the continuous steel casting process, homo- and heterogeneous reactions occur in the tundish, which result in changes in the quantity and composition of non-metallic inclusions (NMIs). The proper control of the steel motion in the tundish may aid the process of NMI flotation to the slag phase (Zhang, 2006; Wang et al., 2007). The quick elimination of NMIs from the liquid steel shortens the time of NMI residence in the steel, whereby eliminating the NMI growth phenomenon caused by the process of diffusion or non-metallic particle mutual collisions. The liquid steel flow mode depends strongly on the number and type of flow control devices and the location of their installation (Espino-Zarate et al., 2010; Boudjabi et al., 2008). Therefore, any con-

 ISSN 1641-8581

structional modifications to the tundish should be preceded by model studies. It is of particular importance in mathematical model-based model studies to properly select initial and boundary conditions, which should map the actual conditions of the examined process as faithfully as possible. In the literature concerning the use of Computational Fluid Dynamic for the analysis of metallurgical processes there are many studies on the selection of boundary and initial conditions and computational grids (Kumar et al., 2004; Staniewski & Derda, 2005; Jowsa & Cwudziński, 2010). However, each change to the mathematical model will require their revalidation. This paper presents the evaluation of the influence of some conditions and adopted assumptions of the multiphase "mixture" model and the population balance model for the computation of the variation of NMI size distribution in liquid steel as it flows through the tundish. Numerical computations were performed using a commercial computer program, Ansys-Fluent®.

2. CHARACTERIZATION OF THE TEST FACILITY AND TESTING METHODOLOGY

The examination of NMI behaviour in the liquid steel was made for two cases differing in the type of the facility, through which the steel flows continuously together with non-metallic inclusion particles. The first facility (test object) constitutes a fragment of a simplified tundish version. The second one corresponds to the actual geometry of the industrial tundish designed for casting concast slabs. The purpose of the studies on the test object was to verify the preliminary hypotheses concerning the likely influence of some factors, e.g. boundary conditions, on the distribution of non-metallic inclusions. The computational domain for the flow objects under consideration was represented in the form of a spatial grid and executed in the Gambit program. Figure 1 presents both objects: the test object built of 806000 tetrahedral elements and the tundish model (composed of approx. 460000 tetrahedral elements). In the test object (figure 1a), liquid steel flows in at a velocity of 1.79 m/s through a 50 mm inner diameter shroud and flows out through a discharge nozzle of an inner diameter of 50 mm. The facility of 2 m long and 0.5 m wide and is filled with liquid steel up to a height of 0.4 m. Liquid steel flowed into the flow reactor with turbulence defined by the values of k and ε being equal to 0.032041 m^2/s^2 and 0.2294136 m^2/s^3, respectively. The temperature of the liquid metal flowing into the flow reactor was 1823 K.

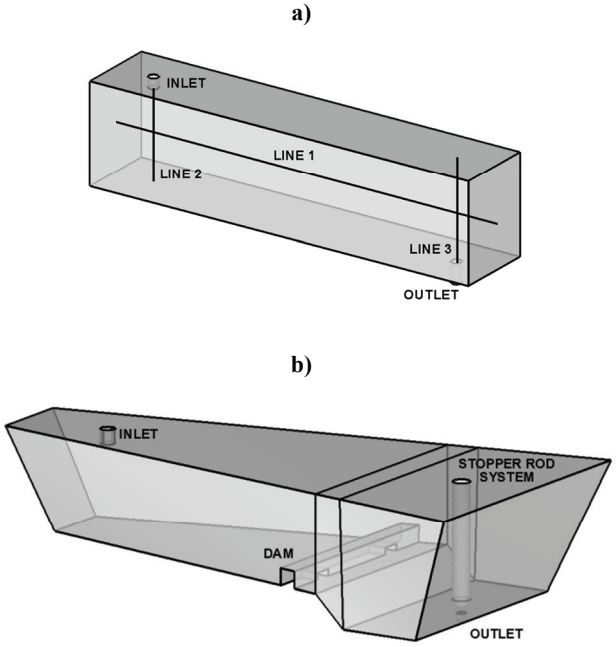

Fig. 1. *Pictorial diagram: a) test flow device and positions of the measurement lines, b) tundish.*

To the tundish (figure 1b), liquid steel flows in at a velocity of 1.3 m/s through a 70 mm inner diameter ladle shroud and flows out through a tundish nozzle of an inner diameter of 70 mm. Liquid steel flowed into the tundish with turbulence defined by the values of k and ε being equal to 0.0169 m^2/s^2 and 0.062771 m^2/s^3, respectively. The temperature of the liquid metal flowing into the tundish was 1823 K. The height of the liquid steel column in the first tundish zone is 0.7 m and 0.9 m in the stopper rod system zone. The nominal capacity of the tundish is 30 Mg. The detailed dimensions of the tundish are given in work (Cwudziński, 2010a). In figure 1a, measurement lines are plotted, along which information on the variation of NMI size distribution in the test object was acquired. In the tundish, on the other hand, the non-metallic inclusion distribution was recorded at two points. The first of them is located at a height of 10 mm from the tundish bottom in the feeding stream axis, and the other is situated in the tundish outlet cross-section. The heat loss on the tundish walls and bottom was assumed to be -2600 W/m^2, and on the flow control device wall describing surfaces and the ladle shroud surfaces, -1750 W/m^2. For simulation with boundary condition “wall” the losses at the free metal table surface are -15000 W/m^2. Whereas for simulation with boundary condition “symmetry” on the free steel

table surface, ideal thermal insulation was assumed, whereby the quantity of heat transferred from the steel to the environment was limited to zero. The heat conductivity and heat capacity of the non-metallic phase and liquid steel were, respectively: 5.5 W/m·K, 1364 J/kg·K, 41 W/m·K, 750 J/kg·K. The coefficient of thermal expansion for liquid steel amounted to 0.0001 K^{-1}.

Numerical simulation of the flow of liquid steel and non-metallic inclusion was performed using the Ansys-Fluent® program. Studies were carried out for five variants, as described in table 1. The first three variants concern the test flow device which was smaller compared to the tundish and had a simplified construction and, in addition, had a denser computational grid, which guaranteed greater accuracy and stability of the system of mathematical equations being solved. The remaining research variants were executed for the facility operating in real industrial conditions.

Table 1. *The research variants examined in the study.*

Research variant number	Test object	Examined boundary condition / discrete phase description	Flow regime	Quantity recorded in the model region
1	Test flow device	Granular and non-granular NMI	Steady and non-isothermal	NMI size distribution curve
2	Test flow device	Symmetry / wall, for free surface of liquid steel	Steady and non-isothermal	NMI size distribution curve
3	Test flow device	Symmetry / wall, for free surface of liquid steel	Unsteady and non-isothermal	RTD E curve
4	Tundish	Symmetry / wall, for free surface of liquid steel	Unsteady and non-isothermal	RTD E curve
5	Tundish	Granular and non-granular NMI	Unsteady and non-isothermal	NMI size distribution curve

For the study of NMI behaviour it was assumed that the non-metallic phase would be represented by the NMI type with a density of 3960 kg/m^3. In the first and the second research variants, the behaviour of NMIs was examined, whose initial distribution (at the tundish inlet) was uniform in character – 6 NMI groups (fractions), each of a fraction of 0.16, and having the following NMI diameters: 1, 1.58, 2.5, 4, 6.3 and 10 μm. The nucleation rate was assumed to be equal to $1\times10^{+10}$ particles/m^3/s, while the diffusion growth rate equal to 1×10^{-07} m/s. The fifth research variant encompassed the examination of the behaviour of NMIs whose initial distribution (at the tundish gate) could be illustrated with a histogram (figure 2). The assumed NMI distribution had a character corresponding to the results of experimental tests carried out on the industrial facility. The experiment was carried out during a sequence of casting 1500×0.225 m concast slabs at a speed of 0.9 m/min. The industrial experiment included the determination of the initial parameters describing the size distribution and chemical composition of NMI in liquid steel. For the description of the initial condition characterizing the NMI distribution in liquid steel in the tundish at the start of the casting sequence it was assumed that the representative sample would be a steel sample taken from the steelmaking ladle immediately prior to the departure from the ladle furnace stand to the CSC machine. Then, after having freely cooled down, the samples were delivered to the laboratory, where, after cutting the samples, surfaces were prepared for analysis using a light microscope Nikon Epiphot 200. Non-metallic inclusions were grouped into three classes according to their size. The first class included 1 μm-size NMI, the second class included NMI sizes from 1 to 3 μm, and the third class, NMI sizes from 3 to 5 μm. Larger non-metallic inclusions were not taken into consideration for the verification of results, since a metallographic analysis had shown a very low occurrence of NMI of a size above 5 μm.

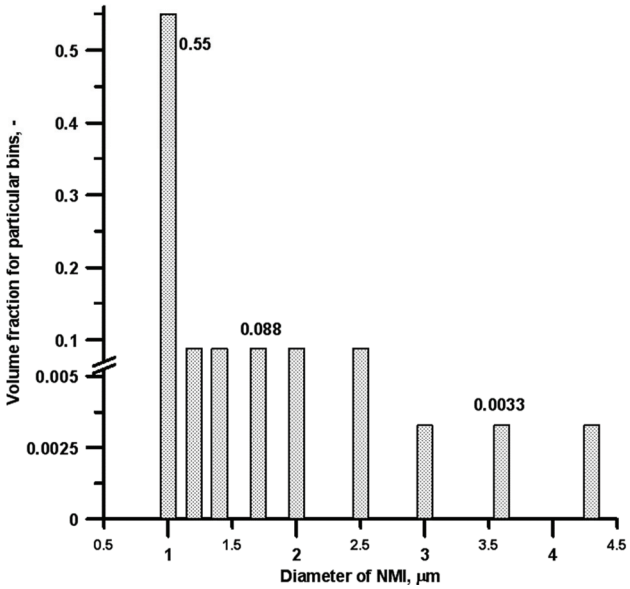

Fig. 2. *Histogram of non-metallic inclusions distribution on the tundish inlet for 5 research variant.*

Additionally, the possibility of homogeneous NMI nucleation was excluded in this variant, and the diffusion growth rate was assumed at a level of 1.7×10^{-07} m/s. In all of the simulation variants, the possibility of NMI aggregation due to turbulent collisions was assumed. In the third and the fourth research variants, an RTD E curve was recorded at the test reactor and the tundish gate, on the basis of which the analysis of the hydrodynamic conditions associated with the flow of steel through the facility was made. Based on the RTD E curve and using the relationships provided by Sahai and Emi (2008), the shares of respective types of flow, i.e. stagnant volume flow, plug flow and ideal mixing flow, were determined.

All five computation variants were investigated aiming at the selection of the most appropriate conditions for the simulation of non-metallic inclusion behaviour under the real conditions of continuous steel casting using the tundish. The first two variants will make it possible to decide on the type of description of the discrete phase ("granular" or "non-granular phase") in liquid steel and evaluate the effect of the boundary condition on the steel free surface ("symmetry" and "wall"). In the multiphase "mixture" model, the "non-granular" model serves for describing particles as being droplets, whereas the "granular" model is used for the description of solid particles. The difference between the aforementioned models lies in the method of describing the exchange of momentum between the dispersed phase and the liquid steel. For the description of interactions between these phases, the interphase exchange coefficient is used, whose general form is represented by the equation below:

$$K = \frac{\alpha \rho_{NMI} f}{\tau} \tag{1}$$

The "granular" and "non-granular" models use different expressions for drag function. The model "granular" makes use of the relationship Schiller and Naumann, while the model „non-granular" model uses the relationship Wen and Yu (Theory Guide, 2009). Variants 3 & 4 are to determine whether or not an effect of changing the boundary condition (from "symmetry" to "wall") for the tundish exists, which would be similar to the one occurring in the test flow reactor in the description of the steel free surface. This is associated with the fact that the "mixture" model employed for describing the phase of non-metallic inclusions in liquid steel with the natural "wall" boundary condition, which enables the representation of the heat exchange with the environment, does not provide the possibility of describing the NMI transition through a boundary set by a given boundary condition. Whereas, the joint use of the "symmetry" condition with a suitable application featuring new user defined functions will provide the capability for secondary phase to flow out from the liquid steel through the free surface (Fluentusers, 2010). On the other hand, however, the "symmetry" condition does not allow for the heat exchange between the tundish and the environment in the form of a heat flux on the free steel table surface. Thus, it is assumed that the tundish has the ideal thermal insulation of the steel free surface and that there is no cooling of the liquid steel through the upper surface. However, this simplification will affect the steel temperature distribution pattern and change to some extent the hydrodynamic conditions in the tundish, which may indirectly determine the behaviour of NMIs.

For the simulation of the simultaneous flow of liquid steel and non-metallic inclusions and growth and aggregation of NMI in the liquid steel, the two-phase "mixture" model with population balance model in the turbulent motion condition was employed (model k-ε). The both model are described by the following equations:

$$\frac{\partial}{\partial t}\left(\rho_m\right)+\nabla\left(\rho_m \vec{v}_m\right)=0 \tag{2}$$

$$\vec{v}_m = \frac{\sum_{k=2}^{2}\alpha_k \rho_k \vec{v}_k}{\rho_m} \tag{3}$$

$$\rho_m = \sum_{k=1}^{2}\alpha_k \rho_k \tag{4}$$

$$\frac{\partial}{\partial t}\left(\rho_m \vec{v}_m\right)+\nabla\left(\rho_m \vec{v}_m \vec{v}_m\right)=-\nabla p+\nabla\left[\mu_m\left(\nabla\vec{v}_m+\nabla\vec{v}_m^{T}\right)\right]+ \rho_m\vec{g}+\vec{F}+\nabla\left(\sum_{k=1}^{2}\alpha_k\rho_k K\vec{v}_{dr,k}\vec{v}_{dr,k}\right) \tag{5}$$

$$\mu_m = \sum_{k=1}^{2}\alpha_k \mu_k \tag{6}$$

$$\vec{v}_{dr,k} = \vec{v}_k - \vec{v}_m \tag{7}$$

$$\frac{\partial}{\partial t}\sum_{k=1}^{2}\left(\alpha_k\rho_k E_k\right)+\nabla\sum_{k=1}^{2}\left(\alpha_k\vec{v}_k\left(\rho_k h_k+p\right)\right)=\nabla\left(k_{eff}\nabla T\right)+S_E \tag{8}$$

The relative velocity and drift velocity are presented by the following expressions:

$$\vec{v}_S = \vec{v}_{NMI} - \vec{v}_{steel} \tag{9}$$

$$c_k = \frac{\alpha_k \rho_k}{\rho_m} \tag{10}$$

$$\vec{v}_{dr,NMI} = \vec{v}_S - \sum_{k=1}^{2} c_k \vec{v}_k \tag{11}$$

The population balance model for NMI is presented by the following expressions:

$$\frac{\partial}{\partial t}(\rho_{NMI}\alpha_i) + \nabla(\rho_{NMI} u_i \alpha_i) + \frac{\partial}{\partial V}\left(\frac{G_v \rho_{NMI}\alpha_i}{V}\right) =$$

$$\rho_{NMI} V_i \left(B_{ag,i} - D_{ag,i}\right) + 0^i \rho_{NMI} V_0 \dot{n}_0 \tag{12}$$

$$\alpha_i = N_i V_i, \quad i = 0,1,...,N-1 \tag{13}$$

$$N_i(t) = \int_{V_i}^{V_{i+1}} n(V,t)dV \tag{14}$$

$$f_i = \frac{\alpha_i}{\alpha_T} \tag{15}$$

$$\frac{\partial}{\partial V}\left(\frac{G_v \rho_{NMI}\alpha_i}{V}\right) = \rho_{NMI} V_i \left[\left(\frac{G_{v,i-1} N_{i-1}}{V_i - V_{i-1}}\right) - \left(\frac{G_{v,i} N_i}{V_{i+1} - V_i}\right)\right] \tag{16}$$

$$B_{ag,i} = \sum_{k=1}^{N}\sum_{j=1}^{N} a_{kj} N_k N_j x_{kj} \xi_{kj} \tag{17}$$

$$D_{ag,i} = \sum_{j=1}^{N} a_{ij} N_i N_j \tag{18}$$

$$a_{ij} = a\left(V_i, V_j\right) \tag{19}$$

$$\xi_{kj} = \begin{cases} 1 \quad for \quad V_i < V_{ag} < V_{i+1}, \quad where \quad i \le N-1 \\ 0 \quad otherwise \end{cases} \tag{20}$$

$$V_{ag} = [x_{kj} V_i + \left(1 - x_{kj}\right) V_{i+1}] \tag{21}$$

$$x_{kj} = \frac{V_{ag} - V_{i+1}}{V_i - V_{i+1}} \tag{22}$$

The variation in the size of NMIs as a result of their mutual collisions caused by the turbulent motion of steel in the population balance model is expressed by the so called collision kernel (a_{ij}) which is described by the following expressions (Population Balance Module Manual, 2009):

$$a_{ij} = \iota_T \sqrt{\frac{8\pi}{15}} \dot{\gamma} \frac{\left(L_i + L_j\right)^3}{8} \tag{23}$$

$$\dot{\gamma} = \frac{\varepsilon^{0,5}}{\nu} \tag{24}$$

$$\iota_T = 0{,}732\left(\frac{5}{N_T}\right)^{0,242} \tag{25}$$

$$N_T = \frac{6\pi\mu\left(L_i + L_j\right)^3 \dot{\lambda}}{8H} \tag{26}$$

$$\dot{\lambda} = \left(\frac{4\varepsilon}{15\pi\nu}\right)^{0,5} \tag{27}$$

3. COMPUTATION RESULTS

From the computer simulations of the process of steel flow through the tundish, characteristics in the form of NMI size distribution curves and liquid steel residence time curves (RTD E) were obtained. The third figure concerns the test object, where computation results for the variation in the share of fractions in respective NMI size groups are shown in the plotted lines. Inclusions described by the "granular" and "non-granular" formalisms were considered. In figures 3a and 3c, very small differences occur between the variants of computation for NMIs in the form of solid and liquid particles. Slightly greater differences in fractions distribution between the NMI types analyzed were observed in the tundish pouring zone (figure 3b). This is probably due to the large velocity and turbulence gradients in the feeding stream axis, and this reflects the state of differentiation of non-metallic particle sizes at the initial stage. The ultimate changes in the size distribution of NMIs in the liquid steel are indicated, however, by the characteristics from figure 3c, as red out for the x coordinate equal to –0.1, which corresponds to the location of the surface situated at the facility's outlet. Looking at these results it can be noticed that the existing differences do not essentially change the NMI size distribution pattern.

Figure 4 presents computer simulation results for the variation in the share of particular NMI group fractions depending on either the "symmetry" or "wall" boundary condition applied on the liquid steel

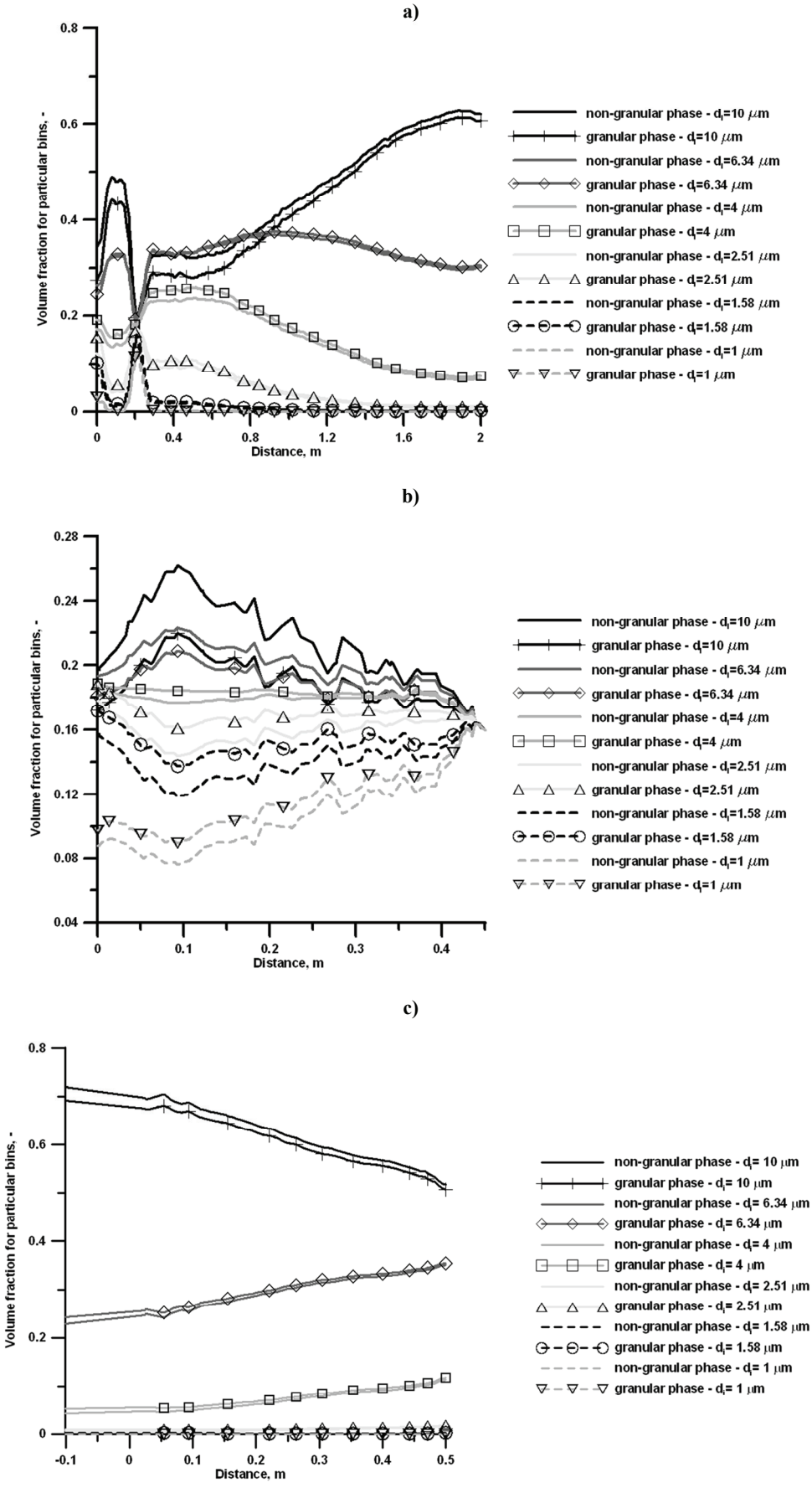

Fig. 3. *Influence of initial conditions for changing of NMI distribution size for each group of NMI: a) on measurement line 1, b) on measurement line 2, c) on measurement line 3.*

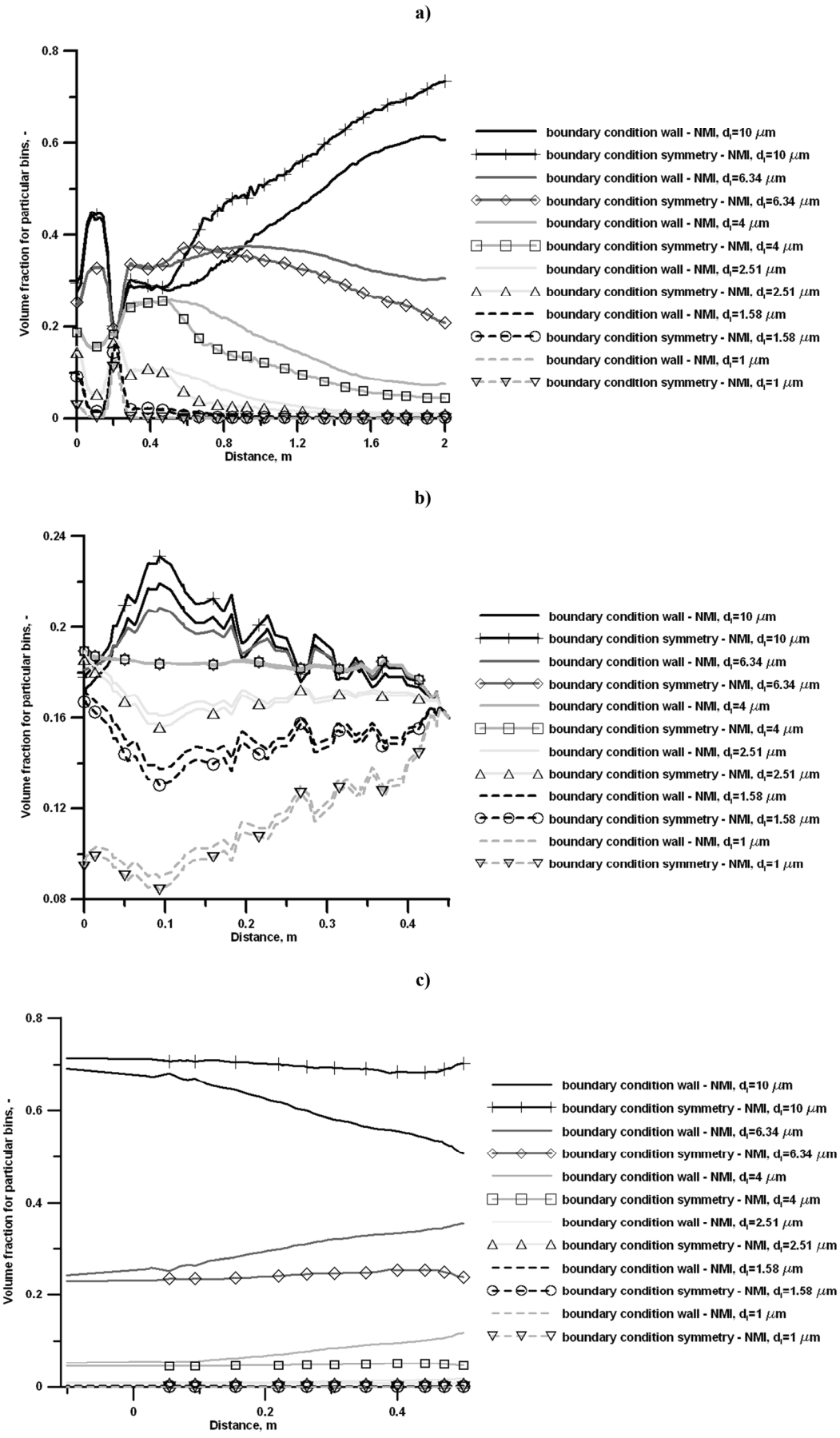

Fig. 4. *Influence of boundary conditions for changing of NMI distribution size for each group of NMI: a) on measurement line 1, b) on measurement line 2, c) on measurement line 3.*

free surface. As the "symmetry" boundary condition does not allow the heat losses from the facility's liquid steel free surface to be expressed, therefore the presented figures show that the change in the thermal state of liquid steel influences the size distribution pattern for particular NMI groups. This is so, because the difference is caused by the effect of the natural convection influencing the steel flow. The observed differences increase with increasing distance from the tundish pouring zone, since the liquid steel flow intensity, which eliminated the convection fluxes associated directly with temperature gradients and steel flow velocity, decreases (figures 4a and 4c). This effect can be observed most clearly at the ends of the line which is situated closest to steel free surface in the facility examined, and very distinctly decreases immediately at the nozzle (the beginning of the line) (figure 3). The effect of the forces of natural convection and the temperature field on the liquid steel flow in the tundish is described in detail in work (Cwudziński & Jowsa, 2008b; Cwudziński, 2010b).

To verify the hypothesis that there is an effect of the type of boundary condition on the steel free surface and on the pattern of steel flow through the facilities under examination, additional tests were carried out (research variant nos. 3 and 4). These consisted in the simulation of tracer motion in the tundish and the flow reactor with simultaneous recording of changes in tracer concentration at the nozzles of the devices under consideration. From Figures 5a and 5b it can be seen that the application of an ideal thermal insulation on the steel table in the form of the "symmetry" boundary condition has resulted in a moderate change in the behaviour of the RTD curve. Based on these characteristics, the magnitudes of changes in particular flow regimes can be assessed. For the test flow reactor, the differences in the shares of plug flow and stagnant volume flow amount to about 5%, whereas for ideal mixing flow the difference is little significant, being 0.4%. For the tundish, the effect of selection of either the "wall" or "symmetry" boundary condition has a slightly different pattern. The differences in the shares of plug flow and stagnant volume flow are, respectively, 3.2% and 1.4%, while for ideal mixing flow this being 4.6%. From these results it can be concluded that the selection of the type of boundary condition has in either case a moderate significance for the evaluation of the motion of steel in the facilities examined.

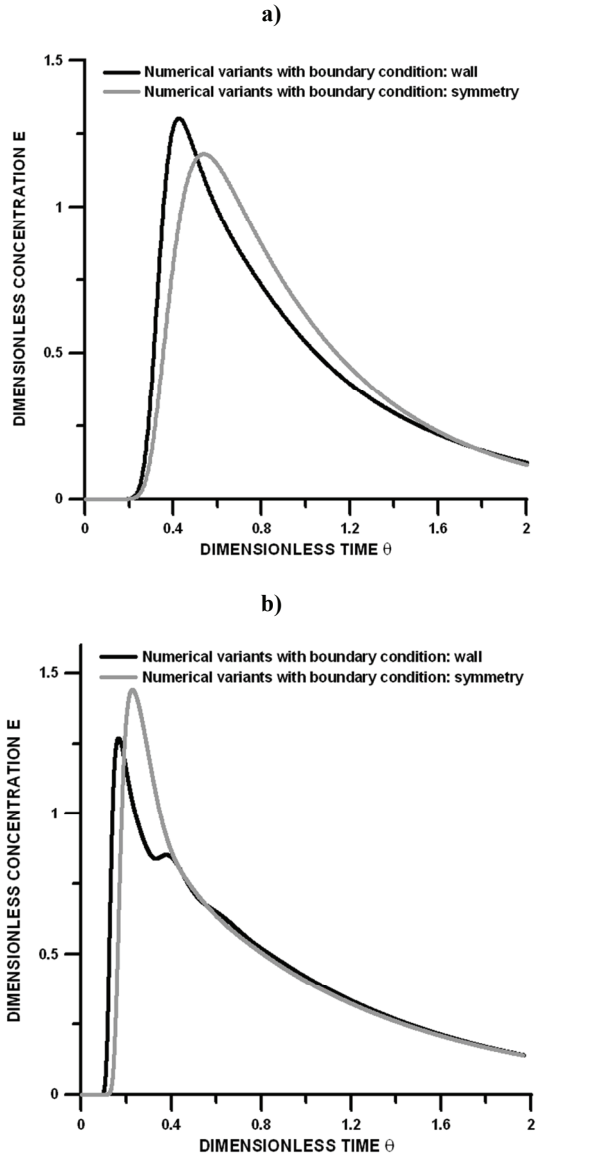

Fig. 5. *Residence time distribution curve: a) flow reactor, b) tundish.*

Table 2. *Flow system for testing facilities.*

Type of flow	Percentage contribution [%]			
	Simulation with boundary condition: wall		Simulation with boundary condition: symmetry	
	Flow reactor	Tundish	Flow reactor	Tundish
Stagnant flow	23.2	34.1	18	35.5
Plug flow	21.3	8.7	26.9	11.9
Ideal-mixing flow	55.5	57.2	55.1	52.6

At the fifth research stage, numerical simulations of NMI behaviour in liquid steel were performed for the tundish, assuming the initial distribution of NMIs corresponding to the conditions prevailing in the industrial plant and, in addition, allowing their transfer through the free surface and floating to the slag (the symmetry and user defined function condi-

tions). Also, two methods of describing the dispersed phase, as either "granular" or "non-granular", were considered in this variant. This was to be the final test for verifying the effect of this description for slightly different steel casting process conditions. Figures 6a and 6b show curves representing the variations in the share of the NMI fraction of a size of 1 μm (figure 6a) and 11 μm (figure 6b). The curves describe the condition for the monitoring point situated in the axis of the tundish feeding stream at a height of 10 mm from the tundish bottom. Figures 7a and 7b, on the other hand, record the variation in the fraction share at the tundish nozzle for the same NMI size groups. Figures 6 and 7 both confirmed the authors' observations that the employed descriptions of the dispersed phase (within the NMI particle size range examined) had no particular significance.

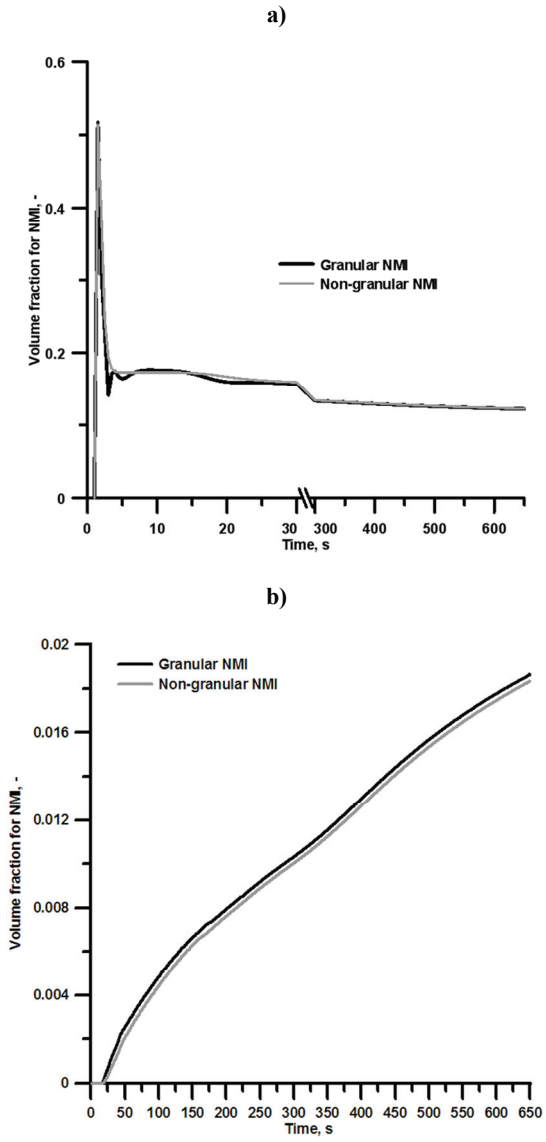

Fig. 6. Change of volume fraction in the tundish pouring zone: a) for 1 μm NMI, b) for 11 μm NMI.

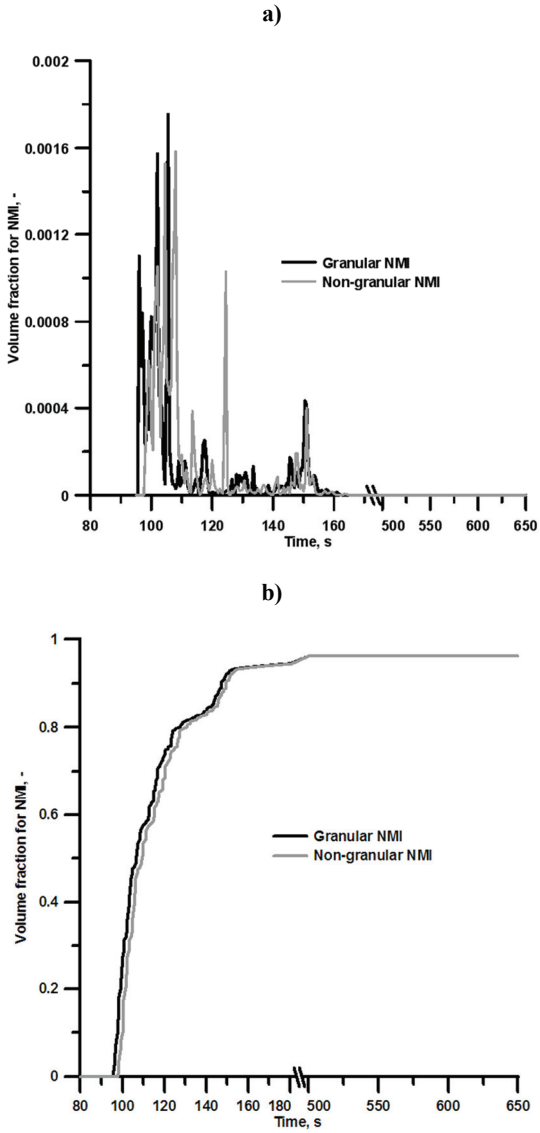

Fig. 7. Change of volume fraction in the outlet tundish: a) for 1 μm NMI, b) for 11 μm NMI.

4. SUMMARY

From the obtained results of computer simulations of liquid steel flow and NMI behaviour it has been found that:

- Computer simulations allow boundary conditions and discrete phase description, being available either directly in the Ansys–Fluent® program or after using user defined function (additional part of numerical code), to be selected so as to achieve a state which is similar to the real conditions prevailing in the tundish during the transport of NMIs and change in their size distribution due to mutual collisions and diffusion growth;
- Employing either the "granular" or "non-granular" model for describing the behaviour of NMIs in the form of a dispersed phase in the

liquid steel does not affect significantly the outcome of the computation of NMI size distribution variation in the facilities examined;

– The selection of either the "symmetry" or "wall" boundary condition on the steel free surface changes the thermal and hydrodynamic conditions of the flowing steel, which is reflected in the shape of the RTD curves for both facilities examined;
– Thus resulted changes in the steel flow regime (stagnant volume flow, plug flow, or ideal mixing flow) do not exceed the share of 5%. This causes small changes in NMI size distribution in the examined regions of the test object and the tundish;
– The proposed mathematical model only lacks the description of the complex mechanism of NMI transition through the interface and NMI assimilation in the slag phase.

The obtained investigation results constitute a very valuable experience gained in attempting to evaluate the complex phenomena associated with the behaviour of non-metallic inclusions during continuous casting of steel using a tundish. However in the future population model will be verified via industrial experiment. Aim of industrial experiment will be selection of suitable NMI growth mechanism to describe precisely behaviour of non-metallic inclusions in the liquid steel flowed through the tundish during continuous steel casting.

NOMENCLATURE

a_{ij}	aggregation kernel [m^3/s]
$B_{ag,\,i}$	NMI size i birth rates of aggregation [m^3/s]
c_k	mass fraction for any phase k [-]
$D_{ag,\,i}$	NMI size i death rates of aggregation [m^3/s]
f	drag function [-]
f_i	fraction of α [-]
$\vec{F}$	body force [N]
g	gravitational acceleration [m/s^2]
G_v	particle volume [m^3]
h_k	enthalpy for phase k [J/kg]
H	Hamaker constant for non-metallic inclusions 2,3·10^{-20} [J]
k_{eff}	effective thermal conductivity [W/m·K]
k	type of phase: 1 – liquid steel; 2 – non-metallic inclusions
L	characteristic dimension of NMI [m]
n	number of phases [-]
$\dot{n}_0$	nucleation rate [particles/m^3/s]
N	number of bins [-]
N_T	ratio between viscous force and Van der Waals force [-]
p	pressure [Pa]
S_E	volumetric heat sources
T	temperature [K]
t	time [s]
u_i	velocity magnitude of NMI size i [m/s]
$\vec{v}_{dr,k}$	drift velocity of phase k [m/s]
$\vec{v}_m$	mass averaged velocity [m/s]
$\vec{v}_k$	velocity of phase k [m/s]
$\vec{v}_S$	slip velocity [m/s]
$\vec{v}_{NMI}$	velocity of NMI [m/s]
$\vec{v}_{steel}$	velocity of liquid steel [m/s]
$\vec{v}_{dr,NMI}$	drift velocity of NMI [m/s]
$\vec{v}_k$	velocity of phase k [m/s]
V	volume [m^3]
V_i	volume of the NMI size i [m^3]
V_{ag}	NMI volume resulting from the aggregation of NMI *k* and *j* [m^3]
x_{kj}	contribution of particle k and j [-]
ρ_k	density of phase k [kg/m^3]
ρ_m	mixture density [kg/m^3]
ρ_{NMI}	density of non-metallic inclusions [kg/m^3]
μ_m	viscosity of mixture [Pa·s]
μ_k	viscosity of phase k [Pa·s]
τ	particulate relaxation time [s]
α_i	volume fraction of particle size I [-]
α_k	volume fraction of phase k [-]
α_{NMI}	volume fraction of the NMI [-]
α_T	total volume fraction of the NMI [-]
ι_T	empirical capture efficiency coefficient of turbulent collision [-]
$\dot{\gamma}$	shear rate [1/s$^{0.5}$·m]
ε	turbulent energy dissipation rate [m^2/s^3]
ν	kinematic viscosity [m^2/s]
$\dot{\lambda}$	deformation rate [1/s]

ACKNOWLEDGEMENTS

This scientific work has been financed from the resources allocated for Science in the years 2009-2011 as Research Project No. N508390437.

This publication has been made with the financial support by the Foundation for Polish Science.

REFERENCES

Ahn, T.-S., Lee, K.-H., Lee, K.-H., Park, H.-S., 2007, Tundish Shape Design using Numerical Approximate Solution, *Numerical Analysis and Applied Mathematics, Int. Conf.,* ed. T.E. Simos, 41-44.

Boudjabi, A. F., Bellaouar, A., Lachi, M., Dumortier, C., 2008, *4th Int. Conf. On Applied and Theoretical Mechanics,* Cairo, 26-31.

Cwudziński, A., Jowsa, J., 2008a, Numerical modeling of influence of gaseous bubble shape factor on steel flow in the tundish with system of argon injection, *Computer Method in Materials Science,* 8, 16-24.

Cwudziński, A., Jowsa, J., 2008b, Numerical Analysis of Steel Flow in the Six-strand Tundish with Sublux Controller of turbulence, *Archiv. Metall. Mater.,* 53, 749-760.

Cwudziński, A., 2010a, Numerical Simulation if Liquid Steel Flow in Wedge-type One-strand Slab Tundish with a Subflux Turbulence Controller and an Argon Injection System, *Steel Res. Int.,* 81, 123-131.

Cwudziński, A., 2010b, Wpływ urządzeń sterujących przepływem ciekłej stali w kadzi pośredniej na konwekcję naturalną, *Hutnik – Wiadomości Hutnicze,* 77, 204-207 (in polish).

Espino-Zarate, A., Morales, R. D., Najera-Bastida, A., Macias-Hernandez, M. J., Sandoval-Ramos, A., 2010, Fluid flow and Mechanisms of Momentum Transfer in a Six-Strand Tundish, *Metall. Mater. Trans.* B, 41B, 962-975.

Fluentusers, 2010. *2002-5 Fluent Germany GmbH*, Jochen Schuetze, User Defined Function. Available online at: www.fluentusers.com.

Jowsa, J., Cwudziński, A., 2010, Influence of Turbulence Models on Steel Flow Character in the Tundish, *Archiv. Metall. Mater.*, 55, 477-488.

Kumar, A., Koria, S. C., Mazumdar, D., 2004, An Assessment of Fluid Flow Modelling and Residence Time Distribution Phenomena in Steelmaking Tundish Systems, *ISIJ Int.*, 44, 1334-1341.

Liu, S.-x., Yang, X.-m., Du, L., Li, L., Liu, C.-z., 2008, Hydrodynamic and Mathematical Simulation of Flow Field and Temperature Profile in an Asymmetrical T-type Single-strand Continuous Casting Tundish, *ISIJ Int.*, 48, 1712-1721.

Population Balance Module Manual, 2009, *Ansys-Fluent® 12.0*.

Sahai, Y., Emi, T., 2008, *Tundish Technology for Clean Steel Production*, World Scientific Publishing Co., 99-127.

Staniewski, I., Derda, W., 2005, Application of the CFD Computing Technique to Numerical Modeling of Continuous Casting of Steel, *Archiv. Metall. Mater.,* 50, 843-856.

Theory Guide, 2009, *Ansys-Fluent® 12.0*.

Wang, Y., Wen, G., Tang, P., Zhu, M., Chen, Y., Song, W., 2007, Mathematical modeling of Fluid Flow, Heat Transfer and Inclusions Transport in a Four Strand Tundish, *J. Univ. Sci. Technol. Beijing,* 14, 22-26.

Zhang, L., 2006, Fluid Flow, Heat Transfer and Inclusion Motion in molten Steel Continuous Casting Tundish, *5th Int. Conf. On CFD in the Process industries CSIRO,* Melbourne, 1-11.

Zhong, L. C., Li, L. Y., Wang, B., Zhang, L., Zhu, L. X., Zhang, Q. F., 2008, Fluid Flow Behaviour in Slab Continuous Casting Tundish with Different Configurations of Gas Bubbling Curtain, *Ironmaking Steelmaking,* 35, 436-440.

ZASTOSOWANIE MODELU BILANSU POPULACJI DLA PRZEWIDYWANIA ZACHOWANIA SIĘ WTRĄCEŃ NIEMETALICZNYCH W CIEKŁEJ STALI

Streszczenie

Artykuł przedstawia wyniki symulacji komputerowej przepływu stali w jednootworowej kadzi pośredniej wyposażonej w niską przegrodę. Autorzy wykorzystali technikę modelowania numerycznego CFD (Computational Fluid Dynamics) dla pokazania wpływu różnych wariantów warunków brzegowych i początkowych na wynik symulacji numerycznej przepływu stali i zachowania się wtrąceń niemetalicznych (WN). Symulacje były wykonane dla warunków nieizotermicznych, stacjonarnych i niestacjonarnych. Do przewidywania zachowania się wtrąceń niemetalicznych w ciekłej stali zastosowano model „mixture" i model „bilansu populacji". W efekcie obliczeń otrzymano krzywe rozkładu wielkości WN, krzywe RTD oraz udziały procentowe poszczególnych stref przepływu (przepływ stagnacyjny, tłokowy i idealnego mieszania).

Submitted: February 11, 2011
Submitted in a revised form: April 11, 2011
Accepted: June 22, 2011